Steel and Composite Structures, *Vol. 27, No. 6 (2018) 777-788*
DOI: https://doi.org/10.12989/scs.2018.27.6.777

Thermal buckling of FGM beams having parabolic thickness variation and temperature dependent materials

Othman Arioui [1,2], Khalil Belakhdar [*3,5], Abdelhakim Kaci [4,5] and Abdelouahed Tounsi [5,6]

[1] *Department of Civil Engineering, University of Oran of Science and Technology, Oran, Algeria*
[2] *Laboratory of Structural Mechanics and Structural Stability, University of Oran of Science and Technology, Oran, Algeria*
[3] *Department of Science and Technology, University Centre of Tamanrasset, BP 10034 Sersouf, Tamanrasset, Algeria*
[4] *Department of Civil Engineering and Hydraulics, University of Saida, Algeria*
[5] *Laboratory of Materials and Hydrology, University of Sidi Bel Abbes, Algeria*
[6] *Department of Civil and Environmental Engineering, King Fahd University of Petroleum & Minerals, 31261 Dhahran, Eastern Province, Saudi Arabia*

(*Received February 26, 2018, Revised March 29, 2018, Accepted April 6, 2018*)

Abstract. An investigation on the thermal buckling resistance of simply supported FGM beams having parabolic-concave thickness variation and temperature dependent material properties is presented in this paper. An analytical formulation based on the first order beam theory is derived and the governing differential equation of thermal stability is solved numerically using finite difference method. a function of thickness variation is introduced which controls the parabolic variation intensity of the beam thickness without changing its original material volume. The results showed the high importance of taking into account the temperature-dependent material properties in the thermal buckling analysis of such critical beam sections. Different Influencing parametric on the thermal stability are studied which may help in design guidelines of such complex structures.

Keywords: FGM beam; thermal buckling; stability analysis; finite difference method; parabolic-concave; thickness variation

1. Introduction

In recent years, functionally graded materials (FGMs) have received a considerable attention in several engineering and industries applications due to its high performance and resistance in aggressive and high temperature environments. This type of composite materials is characterized by its properties that vary smoothly through the thickness. Generally, FGM are composed of metal and ceramic where the smoothness can be performed by gradually varying the volume fraction of the constituent materials (Ahmed 2014, Akavci 2015, Kar and Panda 2015, Shahsavari *et al*. 2018). Such operation results in a mixture that can operate well under high mechanical and thermal loads.

A number of pieces of research work have been conducted to study the buckling behavior of FGM structures under mechanical and/or thermal loading by adopting different theories and assumptions (Nami *et al*. 2015, Karami *et al*. 2018b, Panda and Katariya 2015), where, various cases of loading and boundary conditions have been extensively studied. Akbaş (2015) and Hadji *et al*. (2017) investigated wave propagation of a functionally graded beam in thermal environments using various higher-order shear deformation beams theories. Karami *et al*. (2017a-b, 2018a) also studied the wave propagation but in nano-plates. Recently, Kolahchi and his co-authors (Kolahchi and Bidgoli 2016, Kolahchi *et al*. 2016a, b, Kolahchi 2017, Kolahchi and Cheraghbak 2017, Kolahchi *et al*. 2017a-c, Hajmohammad *et al*. 2017) and Shokravi (Shokravi 2017a-d) presented many pieces of research work where they extensively studied and analyzed the stability of different types of structures under various conditions and materials properties. They adopted different nonlocal theories and constitutive material properties to study the mechanical and thermal behavior of nano-tubes and plates. In other research works (Arani and Kolahchi 2016, Bilouei *et al*. 2016, Zamanian *et al*. 2017), the researchers studied the buckling of concrete columns strengthened with nano fibes and tubes. Aydogdu (2006) presented an analytical formulation based on three degrees of freedom shear deformable beam theory to analyze buckling of cross-ply laminated beams with different boundary conditions. The derived governing equations are obtained by using the principal of Minimum Energy and the critical buckling load are evaluated through using Ritz method. Shahsiah *et al*. (2009) presented an analytical procedure based on the one-dimensional theory of elasticity. They derived the stability equation through using the variational and force summation method. In their work, Kiani and his co-authors (Kiani and Eslami 2010) analyzed the thermal buckling of FGM beams under different types of temperature distribution through the thickness. They examined the existence of bifurcation type buckling in terms of type of thermal loading and boundary conditions. Huang and Li (2010) carried out a research

∗Corresponding author, Professor,
E-mail: be.khalil@gmail.com

http://www.techno-press.org/?journal=scs&subpage=6
ISSN: 1229-9367 (Print), 1598-6233 (Online)

work on the stability analysis of circular cylindrical columns and beams made of functionally graded materials by including different shear deformation theories. Wattanasakulpong *et al*. (2011) investigated the thermal buckling in addition to elastic vibration of FGM beams based on an improved third-order shear deformation theory. They studied the beams under different types of immovable boundary conditions with temperature dependent material properties. Yazdani *et al*. (2011) studied the buckling of laminated composite beams having piezoelectric layers exposed to uniform type of thermal loading and constant voltage. Their formulation is based on the first order shear deformation theory. They studied the effect of different sets of boundary conditions, actuator voltage, and beam geometry on the critical buckling temperature. Fallah and Aghdam (2012) presented a piece of research work to investigate the thermo-mechanical buckling and nonlinear free vibration of FGM beams on nonlinear elastic foundation. Their formulations have been derived based on Euler–Bernoulli assumption and they used Von Karman to establish the nonlinear strain–displacement relation. After solving the governing equation, they conducted a parametric analysis to study the effect of different parameters on the buckling as well as the vibration characteristics of FGM beams. Kiani and Eslami (2013) studied the Thermomechanical buckling of FGM with different boundary conditions and exposed to diverse types of thermal loading variation across the thickness by considering that the material properties are temperature dependent. Anandrao and his co-authors (Anandrao *et al*. 2013) studied the effect of analyzing FGM beams with temperature dependent materials properties on the critical thermal buckling. They used finite element based on the first-order shear deformation theory element. Bouazza *et al*. (2014) studied the nonlinear post-buckling response of composite beams based on higher-order shear deformation theories. They investigated the effects of temperature and moisture concentrations on the general post-buckling of the beam with restrained supports from axial movement. Bennai and his co-authors (Bennai *et al*. 2015) developed a new hyperbolic shear and normal deformation beam theory using the refined concept in order to study the free vibration and buckling of simply supported FGM sandwich beams. Mohammadabadi *et al*. (2015) analyzed the buckling of micro composite laminated beams exposed to thermal loading based on different beam theories. They studied the effect of boundary conditions and cross ply laminate on the critical temperature. In a research work presented by Sun *et al*. (2016), a numerical method named shooting method was used to study the thermal buckling and post-buckling thermomechanical behavior of FGM beam resting on a two-parameter non-linear elastic foundation. They studied also the influence of different geometric and material properties.

It should be stated that, FGM structures having complex geometric properties have also attracted the attention of designers and researchers (Janghorban and Rostamsowlat 2012, Kar and Panda 2016, 2017, Katariya and Panda 2016, Katariya *et al*. 2017, Madani *et al*. 2016, Panda and Singh 2009, 2010, 2013a-c). In this context, the use of beams and plates with variable thickness becomes common in different engineering and industrial fields due to the design requirements. In spite of that, pieces of research work carried out to study the buckling of FGM beams with variable thickness are few. Generally, introducing such features like thickness variation in an analytical solution leads to complex equations (Atmane *et al*. 2011, Jabbarzadeh *et al*. 2013, De Faria and De Almeida 2004, Pouladvand 2009, Mozafari *et al*. 2010, Mozafari and Ayob 2012, Siddiqui 2015, Ghayesh and Farokhi 2018). This problem pressed many researchers to use numerical methods to simplify the analysis of beams or plates with complex geometry. Panda and his co-authors (Panda and Singh 2010, 2013b, d, Panda and Katariya 2015) worked on the buckling and vibration of different shapes of laminatd composite panels under thermal conditions using the finite element method. Rajasekaran and Wilson (2013) used the finite difference method to evaluate the exact buckling loads and vibration frequencies of variable thickness isotropic plates under different combinations of boundary conditions and loading. In their work, Ghomshei and Abbasi (2013) presented a numerical method by using finite element method to analyze the thermal buckling of FGM annular plates with a variable thickness. Bouguenina *et al*. (2015) used a numerical solution to investigate the thermal buckling behavior of simply supported FGM plates having variable thickness. An analytical formulation was evaluated and solved using finite difference method to include the thickness variation. Different geometrical and mechanical properties were investigated to evaluate their effect on the critical buckling of FGM plates having linear variable thickness.

The objective of the preset work is to study the thermal buckling resistance of FGM beams having parabolic-concave thickness variation. To attend this objective, the derived governing equation of the thermal stability is solved numerically by using the finite difference method in order to have the ability to include the thickness variation. A special parabolic-concave function is developed to control the variation intensity of the beam thickness without changing its original material volume. A parametric study is conducted to investigate the effect of different material ad geometric parameters on the thermal buckling resistance loss.

2. Theoretical formulation

2.1 Material constitutive relations

We consider a functionally graded beam composed of a mixture of ceramics and metals. It is assumed that the composition properties of FGM vary through the thickness of the beam according to a simple power-law function. The volume fractions of ceramic V_c and metal V_m are given by

$$\begin{cases} V_c = \left(\dfrac{z}{h} + \dfrac{1}{2}\right)^k \\ V_m(z) + V_c(z) = 1 \end{cases} \tag{1}$$

h is the beam thickness, k is a parameter that controls

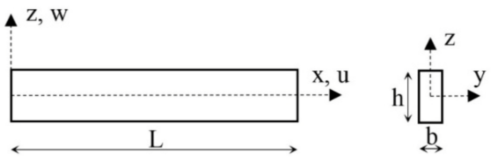

Fig. 1 Coordinate system and geometry of the beam

the material variation profile, where $0 < k < \infty$. In case $k = 0$ represents a full ceramic beam, while $k = \infty$ means that the beam is fully metallic. The modulus E and the coefficient of thermal expansion α are expressed by the following equations

$$\begin{cases} E(z) = E_c V_c + E_m(1 - V_c) \\ \alpha(z) = \alpha_c V_c + \alpha_m(1 - V_c) \end{cases} \tag{2}$$

2.2 Formulation of the stability equations

The FGM beam has a length of L and rectangular cross section $b \times h$. The displacement of a general point in the beams x, z directions denote $\overline{u}(x,z)$ and $\overline{w}(x,z)$, respectively, as shown in Fig. 1.

On the basis of the displacement field given in Eq. (1), Eq. (3) becomes

$$\begin{cases} \overline{u}(x,z) = u_0 + z\phi(x) \\ \overline{w}(x,z) = w_0 \end{cases} \tag{3}$$

Where u_0 and w_0 are displacements of the neutral axis of the beam, $\phi(x)$ is the rotation of the beam cross-section.

The axial and shear strains in the beam are expressed as

$$\begin{cases} \varepsilon_{xx} = \overline{u},_x + \dfrac{1}{2}(\overline{w},_x)^2 \\ \gamma_{xz} = \overline{u},_z + \overline{w},_x \end{cases} \tag{4}$$

Substituting Eq. (3) in Eq. (4) gives

$$\begin{aligned} \varepsilon_{xx} &= u,_x + \frac{1}{2}(w,_x)^2 + z\phi,_x \\ \gamma_{xz} &= \phi + w,_x \end{aligned} \tag{5}$$

The corresponding axial and shear stresses are as follows

$$\begin{cases} \sigma_{xx} = E(\varepsilon_{xx} - \alpha.\Delta T) \\ \tau_{xz} = \dfrac{E}{2(1+\nu)}\gamma_{xz} \end{cases} \tag{6}$$

Eq. (6) may be developed as

$$\begin{aligned} \sigma_{xx} &= E\left[u,_x + \frac{1}{2}(w,_x)^2 + z\phi,_x - \alpha.\Delta T\right] \\ \tau_{xz} &= \frac{E}{2(1+\nu)}(\phi + w,_x) \end{aligned} \tag{7}$$

The forces and moments developed from the stresses components through the thickness are given as Robert (2006)

$$\begin{cases} N_x = \displaystyle\int_{-h/2}^{h/2} \sigma_{xx}\, dz \\ M_x = \displaystyle\int_{-h/2}^{h/2} \sigma_{xx}\, z\, dz \\ Q_{xz} = K_s \displaystyle\int_{-h/2}^{h/2} \tau_{xz}\, dz \end{cases} \tag{8}$$

Where K_s is the shear correction factor which equals to 5/6 for rectangular cross-section (Kiani and Eslami 2013).

Substituting Eq. (7) into Eq. (8), the forces can be expressed as

$$\begin{cases} N_x = E_1\left(u,_x + \dfrac{1}{2}(w,_x)^2\right) + E_2\phi,_x - N_x^T \\ M_x = E_2\left(u,_x + \dfrac{1}{2}(w,_x)^2\right) + E_3\phi,_x - M_x^T \\ Q_{xz} = \dfrac{E_1 K_s}{2(1+\nu)}(\phi + w,_x) \end{cases} \tag{9}$$

Where

$$(E_1, E_2, E_3) = \int_{-h/2}^{h/2} (1, z, z^2) E(z)\, dz \tag{10}$$

$$(N_x^T, M_x^T) = \int_{-h/2}^{h/2} (1, z) E(z) \alpha(z) \Delta T\, dz \tag{11}$$

By using the principle of minimum total potential energy, the derived governing equations for the displacement field given in Eq. (3) are (Kiani and Eslami 2013)

$$\begin{cases} N_{x,x} = 0 \\ M_{x,x} - Q_{xz} = 0 \\ Q_{xz,x} + N_x . w_{,xx} = 0 \end{cases} \tag{12}$$

To derive the stability equations, the adjacent-equilibrium criterion is used. Thus, by assuming that the equilibrium state of the FGM beam is defined in terms of the displacement components u_0, w_0 and ϕ_0 and the displacement components of a neighboring stable state is defined by u_1, w_1 and ϕ_1 with respect to the equilibrium position. Therefore, the total displacements of a neighboring state are given by

$$\begin{cases} u = u_0 + u_1 \\ w = w_0 + w_1 \\ \phi = \phi_0 + \phi_1 \end{cases} \tag{13}$$

Similarly, the force and moment of a neighboring state may be related to the state of equilibrium as

$$\begin{cases} N_x = N_{x0} + N_{x1} \\ M_x = M_{x0} + M_{x1} \\ Q_{xz} = Q_{xz0} + Q_{xz1} \end{cases} \tag{14}$$

Manipulating Eqs. (12)-(14), the resulting reduced equation after satisfying the equilibrium conditions and elimination of u_1, w_1 and ϕ_1, is given as (Kiani and Eslami 2013)

$$w_{1,xxxx} + \lambda^2 w_{1,xx} = 0 \tag{15}$$

where

$$\lambda^2 = \frac{E_1 N_{x0}}{(E_1E_3 - E_2^2)\left(1 - 2N_{x0}\frac{1+\nu}{E_1K_s}\right)} \tag{16}$$

3. Finite difference solution

The fourth order differential equation presented by Eq. (15) can be solved numerically using finite difference method. To do that, we consider an FGM beam divided into n nodes spaced by Δh in x direction, as shown in Fig. 2.

The governing equation given by Eq. (15) may be expressed in finite difference format at node "i" as

$$\begin{aligned} & w_{1_{(i+2)}}\left(\frac{1}{\Delta x^2}\right) + w_{1_{(i+1)}}\left(-\frac{4}{\Delta x^2}+\lambda^2\right) \\ & + w_{1_{(i)}}\left(\frac{6}{\Delta x^2} - 2\lambda^2\right) + w_{1_{(i-1)}}\left(-\frac{4}{\Delta x^2}+\lambda^2\right) \\ & + w_{1_{(i-2)}}\left(\frac{1}{\Delta x^2}\right) = 0 \end{aligned} \tag{17}$$

This mesh is applied at nodes with coordinates $(i = 2..n-1)$. Noting that this operation will result virtual nodes ("-1" and "$n+1$"). These virtual nodes can be eliminated by using the boundary conditions as follows:

For simply supported edges, we have

$$\begin{cases} w_{1_{(i)}} = 0 \\ M_{1_{(i)}} = 0 \end{cases} \tag{18}$$

with $i = (1, n)$ for left edge and right edge, respectively.

Since we have

$$M_{(i)} = \frac{d^2 w_1}{dx^2} = \frac{1}{\Delta x^2}\left(w_{1_{(i+1)}} - 2w_{1_{(i)}} + w_{1_{(i-1)}}\right) \tag{19}$$

When using the condition given in Eq. (18), it results

$$w_{1_{(i+1)}} = -w_{1_{(i-1)}} \quad ; \quad i = 1, n \tag{20}$$

Eq. (20) is used in Eq. (17) for nodes $i = (1, n)$ to eliminate the virtual nodes resulting the following system of simultaneous equations

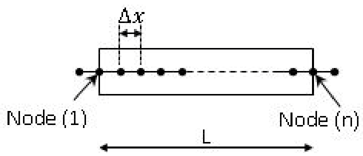

Fig. 2 Finite difference mesh of the beam

3.1 Determination of the critical temperature

The beam is assumed to have an initial uniform temperature T_i. The temperature is raised uniformly through the thickness to a final value T_f in which the beam buckles.

The buckling temperature difference is simply defined as

$$\Delta T = T_f - T_i \tag{22}$$

Where the produced pre-buckling normal force due to thermal loading is

$$N_{x0} = -N_x^T \tag{23}$$

From Eq. (23), Eq. (11) and Eq. (15), the temperature difference ΔT is found as

$$\Delta T = -\frac{E_1(E_1E_3 - E_2^2)w_{1,xxxx}\,.K_s}{P_0\left(-E_1^2.\,w_{1,xx}K_s + 2(EE)w_{1,xxxx}\,(1+\nu)\right)} \tag{24}$$

Where

$$P_0 = \int_{-h/2}^{h/2} E(z)\alpha(z)\,dz \tag{25}$$

$$w_{1,xxxx} = \frac{1}{\Delta x^4}\left(w_{1(i+2)} - 4w_{1(i+1)} + 6w_{1(i)} - 4w_{1(i-1)} + w_{1(i-2)}\right) \tag{26}$$

$$w_{1,xx} = \frac{1}{\Delta x^2}\left(w_{1_{(i+1)}} - 2w_{1_{(i)}} + w_{1_{(i-1)}}\right) \tag{27}$$

The homogeneous simultaneous equations represented by Eq. (21) cannot be solved because the value of λ^2 is in terms of ΔT which is not known. To resolve this problem, the trial and error technique is used as follows:

- Step (1): In the first trial, an initial value equals to unity is assigned to ΔT. After solving the system of equations, the first mode shape solution of w_1

$$\begin{bmatrix} \left(\frac{5}{\Delta x^2} - 2\lambda^2\right) & -\frac{4}{\Delta x^2}+\lambda^2 & \frac{1}{\Delta x^2} & 0 & \cdots & \cdots & 0 & 0 & 0 \\ -\frac{4}{\Delta x^2}+\lambda^2 & \left(\frac{6}{\Delta x^2} - 2\lambda^2\right) & -\frac{4}{\Delta x^2}+\lambda^2 & \frac{1}{\Delta x^2} & \cdots & \cdots & 0 & 0 & 0 \\ \frac{1}{\Delta x^2} & -\frac{4}{\Delta x^2}+\lambda^2 & \left(\frac{6}{\Delta x^2} - 2\lambda^2\right) & -\frac{4}{\Delta x^2}+\lambda^2 & \cdots & \cdots & 0 & 0 & 0 \\ \vdots & \vdots & \vdots & \cdots & \ddots & \vdots & \vdots & \vdots & \vdots \\ 0 & 0 & 0 & \cdots & \cdots & -\frac{4}{\Delta x^2}+\lambda^2 & \left(\frac{6}{\Delta x^2} - 2\lambda^2\right) & -\frac{4}{\Delta x^2}+\lambda^2 & \frac{1}{\Delta x^2} \\ 0 & 0 & 0 & \cdots & \cdots & \frac{1}{\Delta x^2} & -\frac{4}{\Delta x^2}+\lambda^2 & \left(\frac{6}{\Delta x^2} - 2\lambda^2\right) & -\frac{4}{\Delta x^2}+\lambda^2 \\ 0 & 0 & 0 & \cdots & \cdots & 0 & \frac{1}{\Delta x^2} & -\frac{4}{\Delta x^2}+\lambda^2 & \left(\frac{5}{\Delta x^2} - 2\lambda^2\right) \end{bmatrix} \begin{Bmatrix} w_{1_{(2)}} \\ w_{1_{(3)}} \\ w_{1_{(4)}} \\ \vdots \\ w_{1_{(n-3)}} \\ w_{1_{(n-2)}} \\ w_{1_{(n-1)}} \end{Bmatrix} = \begin{Bmatrix} 0 \\ 0 \\ 0 \\ \vdots \\ 0 \\ 0 \\ 0 \end{Bmatrix} \tag{21}$$

is used to calculate the critical buckling temperature ΔT_{cr_1} defined by Eq. (24).

- Step (2): The obtained ΔT_{cr_1} is used in step (1) for another iteration to solve the simultaneous equations (Eq. (21)) where a new critical temperature difference ΔT_{cr_2} is obtained.
- Step (3): Step (1) and step (2) are repeated successively until the following criteria are violated

$$\left|\frac{\Delta T_{cr_i} - \Delta T_{cr_{i-1}}}{\Delta T_{cr_i}}\right| \leq 10^{-5} \tag{28}$$

It should be noted that in case of temperature independent material properties (TID), the above steps to determine the critical temperature ΔT_{cr} are evaluated using the material properties corresponding to the initial ambient temperature equals to 300 K.

However, in case of temperature dependent material properties (TD), an iterative analysis is used as follows:

- Step (4): First, the critical temperature ΔT_{cr} is evaluated as described by steps (1) to (3) using material properties corresponding to the ambient temperature of $T_i = 300\text{K}$.
- Step (5): Next, The material properties are updated correspondingly to the final temperature $T_f = \Delta T_{cr} + T_i$ and a new iteration following the same flow (steps (1) to (3)) is done to calculate a new ΔT_{cr} corresponding to the new material properties
- Step (6): Step (4) and (5) are repeated until the solution is converged according to the following criteria

$$\left|\frac{\Delta T_{cr_{(mat\ .prop\ \ "i")}} - \Delta T_{cr_{(mat\ .prop\ \ "i-1")}}}{\Delta T_{cr_{(mat\ .prop\ \ "i")}}}\right| \leq 10^{-5} \tag{29}$$

4. Validation of the finite difference method

In order to validate the present numerical method, the predicted critical buckling temperature of FGM beam under uniform temperature rise through the thickness is compared with the literature in case of TID and TD material properties. Since the present procedure is based on the first-order shear deformation theory (FSDT), the predicted results are compared with those of Anandrao *et al*. (2013)

Table 1 Temperature dependent coefficients of material properties (Shen 2009)

Materials		P_0	P_{-1}	P_1	P_2	P_3
ZrO_2	E (MPa)	224.27×10^9	0	-1.371×10^{-3}	1.214×10^{-6}	-3.681×10^{-10}
	α (K^{-1})	12.766×10^{-6}	0	-1.491×10^{-3}	1.006×10^{-5}	-6.778×10^{-11}
	ν	0.2882	0	1.133×10^{-4}	0	0
Ni	E (MPa)	223.95×10^9	0	-2.794×10^{-4}	-3.998×10^{-9}	0
	α (K^{-1})	9.9209×10^{-6}	0	8.705×10^{-4}	0	0
	ν	0.3100	0	0	0	0
SiN_4	E (MPa)	348.43×10^9	0	-3.070×10^{-4}	2.160×10^{-7}	-8.946×10^{-11}
	α (K^{-1})	5.8723×10^{-6}	0	9.095×10^{-4}	0	0
	ν	0.24	0	0	0	0
SUS304	E (MPa)	201.04×10^9	0	3.079×10^{-4}	-6.534×10^{-7}	0
	α (K^{-1})	12.330×10^{-6}	0	8.086×10^{-4}	0	0
	ν	0.3262	0	-2.002×10^{-4}	3.797×10^{-7}	0

Table 2 Dimensionless thermal buckling $\lambda = \Delta T_{cr}\, \alpha_m\, (L^2/h^2)$ for H-H supports

k		L/h					
		100		50		10	
		TID	TD	TID	TD	TID	TD
0	Anandrao *et al*. (2013)	0.553	0.546	0.553	0.525	0.540	0.271
	Present	0.553	0.546	0.553	0.525	0.540	0.270
0.5	Anandrao *et al*. (2013)	0.628	0.621	0.628	0.599	0.613	0.317
	Present	0.627	0.620	0.627	0.598	0.612	0.316
1	Anandrao *et al*. (2013)	0.666	0.658	0.665	0.637	0.649	0.347
	Present	0.664	0.656	0.663	0.635	0.647	0.346
10	Anandrao *et al*. (2013)	0.775	0.770	0.774	0.755	0.756	0.497
	Present	0.775	0.770	0.774	0.755	0.756	0.497

Table 3 Dimensionless thermal buckling $\lambda = \Delta T_{cr}\,\alpha_m\,(L^2/h^2)$ for C-C supports

k		L/h					
		100		50		10	
		TID	TD	TID	TD	TID	TD
0	Anandrao *et al*. (2013)	2.212	2.099	2.206	1.830	2.009	0.548
	Present	2.212	2.098	2.205	1.829	2.008	0.547
0.5	Anandrao *et al*. (2013)	2.507	2.391	2.500	2.106	2.275	0.641
	Present	2.507	2.391	2.499	2.105	2.274	0.641
1	Anandrao *et al*. (2013)	2.653	2.541	2.645	2.258	2.410	0.707
	Present	2.652	2.540	2.644	2.257	2.409	0.706
10	Anandrao *et al*. (2013)	3.096	3.019	3.087	2.808	2.816	1.119
	Present	3.095	3.018	3.086	2.808	2.815	1.118

Table 4 Dimensionless thermal buckling $\lambda = \Delta T_{cr}\,\alpha_m\,(L^2/h^2)$ for C-H supports

k		L/h					
		100		50		10	
		TID	TD	TID	TD	TID	TD
0	Anandrao *et al*. (2013)	1.132	1.101	1.130	1.019	1.071	0.399
	Present	1.132	1.101	1.130	1.019	1.076	0.400
0.5	Anandrao *et al*. (2013)	1.283	1.252	1.281	1.167	1.214	0.467
	Present	1.283	1.251	1.281	1.166	1.219	0.468
1	Anandrao *et al*. (2013)	1.358	1.328	1.356	1.245	1.285	0.514
	Present	1.357	1.327	1.355	1.244	1.291	0.514
10	Anandrao *et al*. (2013)	1.584	1.564	1.582	1.504	1.500	0.781
	Present	1.584	1.563	1.582	1.504	1.507	0.783

where their analytical solution is also based on FSDT.

Assuming FGM beam consists of Zirconia (ZrO_2) and Nickel (Ni) where the variation of the material property $P(T)$ in terms of temperature is given by the following nonlinear function (Shen 2009)

$$P(T) = P_0(P_{-1}T^{-1} + 1 + P_1 T + P_2 T^2 + P_3 T^3) \tag{30}$$

The coefficients P_0, P_{-1}, P_1, P_2, and P_3 are give, in Table 1.

Tables 2, 3, and 4 summarize the dimensionless thermal buckling of FGM beam with Hinged-Hinged (H-H), Clamped-Clamped (C-C), and Hinged-Clamped (H-C) supports, respectively, for different values of material distribution profile parameter k and length-to-thickness ratio $\frac{L}{h}$. To test the convergence of the finite difference solution, the predicted numerical results in these tables are given for different mesh sizes $\left(\frac{L}{\Delta x} = 100, 200, 300, 400\right)$. Additionally, to enhance the accuracy of the predicted results, Richardson's extrapolation formula is adopted, which is expressed as (Szilard 2004)

$$\Delta T_{cr}^{[ex]} = \Delta T_{cr}^{[400]} + \frac{\Delta T_{cr}^{[400]} - \Delta T_{cr}^{[200]}}{2^{\mu} - 1} \tag{31}$$

Where $\Delta T_{cr}^{[ex]}$ is the extrapolated value, $\Delta T_{cr}^{[200]}$ and $\Delta T_{cr}^{[40]0}$ are the values of critical temperature obtained by using mesh size $\frac{L}{\Delta x} = 200$ and $\frac{L}{\Delta x} = 400$, respectively.

$\mu = 2$ is the exponent value which depends on the convergence characteristics of the numerical method.

According to the comparison of the results listed in Tables 2-4, it can be observed that the present results are in excellent agreement with the analytical solution of Anandrao *et al*. (2013), which validate the present numerical method.

5. FGM beam with parabolic thickness variation

As mentioned previously, the objective of this study deals with studying the thermal buckling resistance of simply supported FGM beams having parabolic-concave thickness variation. The thickness is changed according to a function that controls only the parabolic variation intensity while the original beam volume is kept unchanged. To do so, assuming a thickness function $H(x)$ varies according to the following general parabolic expression

$$H(x) = c_0 + c_1 x + c_2 x^2 \tag{32}$$

where c_0, c_1 and c_2 are constants

Let e_0 is the thickness at the mid-span, and e_1 is the thickness at the beam edges, thus, Eq. (32) may be written as

$$H(x) = -\frac{4}{L^2}(e_0 - e_1)(x^2 - L.x) + e_1 \tag{33}$$

The volume of the beam with constant thickness (original beam) is V_0 and its thickness is h. The volume of beam with parabolic thickness variation is V_1. Thus, V_0 and V_1 are expressed as

$$V_0 = L.b.h \tag{34}$$

$$V_1 = L.b\left(\frac{2}{3}(e_0 - e_1) + e_1\right) \tag{35}$$

By maintaining the same volume $V_0 = V_1$, we get

$$e_1 + 2e_0 = 3h \tag{36}$$

By expressing e_1 in terms of e_0 as

$$e_1 = \xi.e_0 \tag{37}$$

Where ξ represents the mid-to-side thickness ratio. Noting that $\xi = 1$ corresponds constant thickness and $\xi > 1$ corresponds to parabolic-concave variation, as shown in Fig. 3.

Substituting Eqs. (36) and (37) into Eq. (33), we obtain the desired function of thickness variation. This function is expressed in terms of one parameter (ξ), which controls the intensity of the parabolic variation as

$$H(x) = \frac{3h}{2+\xi}\left(\frac{4(\xi - 1)}{L^2}x^2 + 1\right) \tag{38}$$

Eq. (38) is expressed in the finite difference at each node (i) as follows

$$h_{(i)} = \frac{3h}{2+\xi}\left(\frac{4(\xi - 1)}{L^2}x_{(i)}^2 + 1\right) \tag{39}$$

5.1 Finite difference considerations

In finite difference idealization of beam with variable thickness, it is assumed that at each discrete $\mathrm{Node}_{(i)}$ the thickness is constant which is simply calculated by substituting the Node's x coordinate in Eq. (39), as illustrated in Fig. 3. In this case, the coordinate $z_{(i)}$ at each $\mathrm{Node}_{(i)}$ varies in its proper domain: $\left[-\frac{h_{(i)}}{2}, \frac{h_{(i)}}{2}\right]$.

Based on that, all the equations containing the thickness parameters h, such as Eqs. (10) and (25), are calculated by using the constant value $h_{(i)}$. Note that, the integration expressions through the thickness are evaluated using trapezoidal rule where the thickness $h_{(i)}$ is divided into 2000 subdivisions.

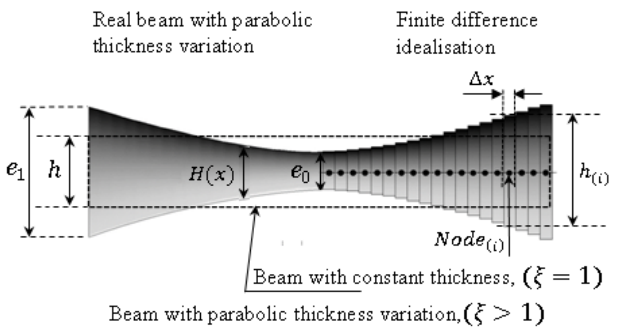

Fig. 3 Finite difference idealisation of FGM beam with parabolic thickness variation

6. Results and discussion

The effect of the parabolic-variation intensity parameter ξ (edge-to-mid thickness ratio) on the critical thermal buckling of simply supported beam is shown in Figs. 4-5. It should be mentioned that all the figures in this

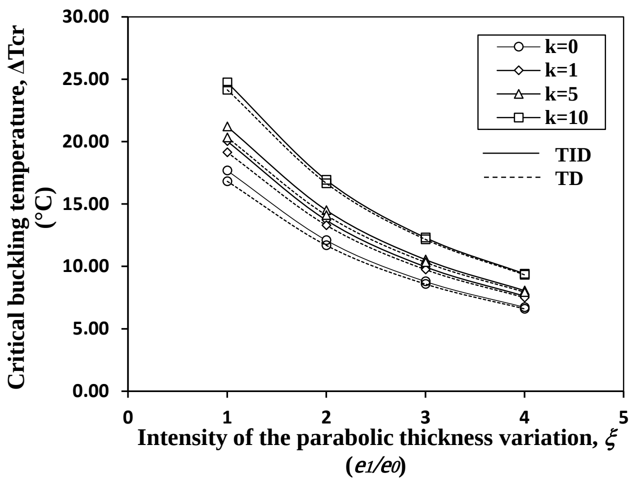

Fig. 4 Critical buckling temperature of simply supported ZrO_2/Ni beam with $L/h = 50$ in terms of the parabolic intensity variation parameter ξ

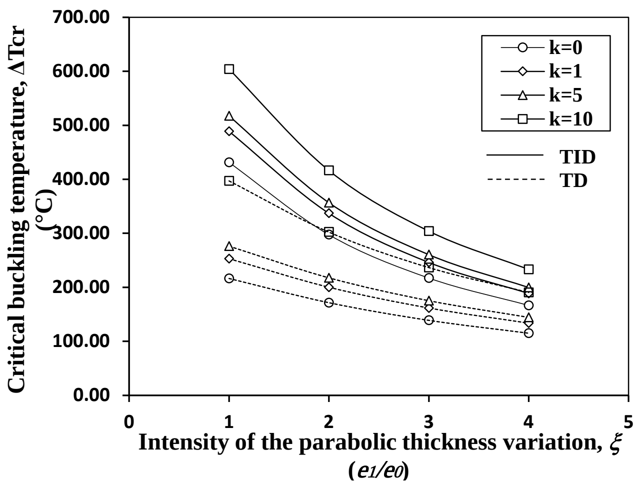

Fig. 5 Critical buckling temperature of simply supported ZrO_2/Ni beam with $L/h = 10$ versus of the parabolic intensity variation parameter ξ

section are given in terms of the thickness h as a reference which represents the original beam thickness, since in beams with variable thickness; both the thickness at the edge and at the mid-span vary with ξ.

These figures show that varying the thickness geometry of the beam to fit a parabolic-concave shape decreases significantly its critical buckling temperature. This is justified by the fact that the increase in the value of ξ helps to the occurrence of buckling since it reduces the thickness at the beam-mid-span where the buckling starts to develop. Besides, it is observed that the material distribution profile affects the critical buckling temperature, where in case of ZrO_2/Ni beam, the lower values of k decrease the beam stiffness and increase its thermal expansion coefficient which motivate the occurrence of the buckling as shown in Fig. 5. However, in case of SiN_4/SUS304 beam (Fig. 6), the lower values of k improve the thermal buckling resistance since they increase the beam stiffness and reduce the thermal expansion coefficient.

From Figs. 4 and 5, it is also observed that, the predicted critical buckling temperatures in case of TID material properties are always higher than the case of TD material properties, noting that the difference of the predicted ΔT_{cr} between the two cases (TID and TD) is grater in thick beam compared to thin beam. This is due to the effect of thermal properties of the constituent materials (thermal expansion coefficients) where as the thickness at the beam-mid-span is big, as the thermal expansion coefficients increases when considering TD compared to the fixed value in case TID. The later reduces considerably the thermal critical temperature. Based on that, neglecting the variation of the material properties due to temperature change leads to an important overestimation of the critical buckling temperature in thick and moderately thick beams with parabolic-thickness variation.

In this section, an investigation is carried out to evaluate the degradation in the thermal buckling resistance of FGM beams when changing the thickness form constant variation to parabolic-concave variation.

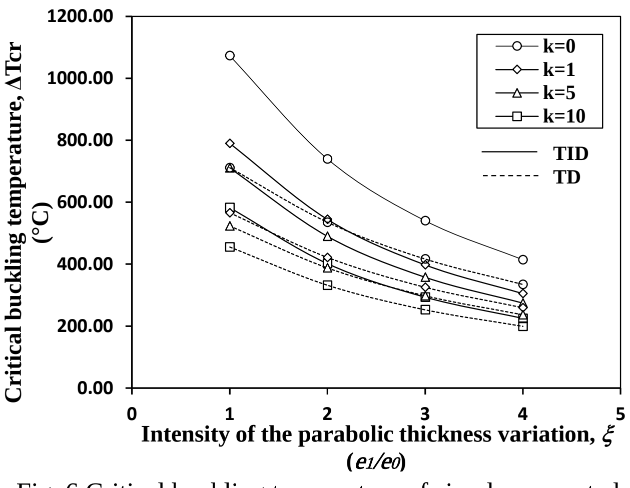

Fig. 6 Critical buckling temperature of simply supported SiN_4/SUS304 beam with $L/h = 10$ versus of the parabolic intensity variation parameter ξ

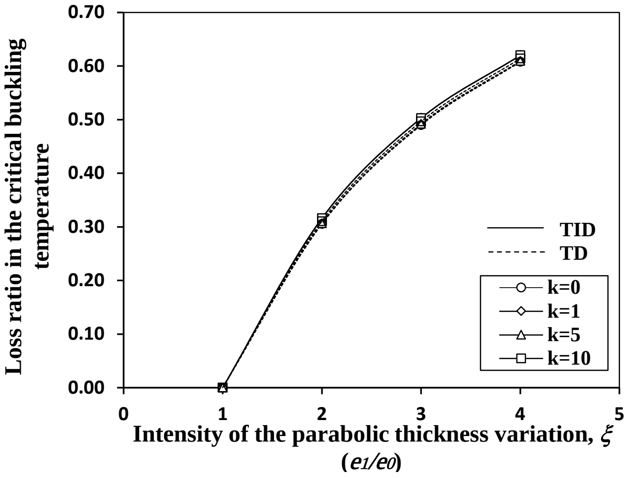

Fig. 7 The loss ratio in the critical buckling temperature versus the parabolic intensity variation parameter ξ in ZrO_2/Ni beam with $L/h = 50$

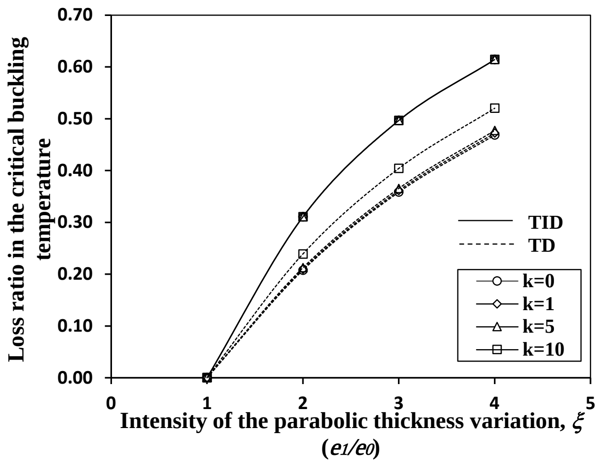

Fig. 8 The loss ratio in the critical buckling temperature versus the parabolic intensity variation parameter ξ in ZrO_2/Ni beam with $L/h = 10$

Figs. 7 and 8 represent the effect of the parabolic thickness variation intensity ξ on the loss ratio of thermal buckling resistance in FGM beams. It is meant by the loss ratio of the buckling resistance; the reduction ratio in the critical buckling load of FGM beam with variable thickness $(\xi > 1)$ with respect to that of the original constant beam thickness $(\xi = 1)$. Noting that the two beams having the same material volume and distribution profile. The loss ratio is simply calculated as follows

$$\text{The loss ratio in } \Delta T_{cr} = \left(\frac{\Delta T_{cr\,(\text{ constant thickness})} - \Delta T_{cr\,(\text{ variable thickness})}}{\Delta T_{cr\,(\text{ constant thickness})}} \right) \tag{40}$$

According to Fig. 7, the results indicate that the increase in the parabolic-variation intensity leads to a significant degradation in the thermal buckling resistance. It is predicted that, the loss ratios of the thermal buckling resistance in thin FGM beams with parabolic-variation intensity of $\boldsymbol{\xi = 2, 3 \text{ and } 4}$ are about 30%, 50%, 60%, respectively, with reference to the original beam with constant thickness $(\boldsymbol{\xi} = \mathbf{1})$.

Besides, the assumption of whether material properties are TD or TID appears to have a negligible effect on the relationship between the loss ratio of the thermal buckling resistance and the parabolic-variation intensity, while the material distribution profile $(\boldsymbol{k})$ found to have no effect.

in case of thick beam, as shown in Fig. 8, the variation of loss ratio of the critical buckling temperature in function of the intensity parameter ξ found to be affected by the material distribution profile only if the material properties are considered TD. Contrariwise, when considering the material properties to be TID, the effect of the material distribution profile found to have an effect on this relationship. These observations illustrate the important role of the thermal expansion coefficients when they are considered temperature dependent especially in thick beams.

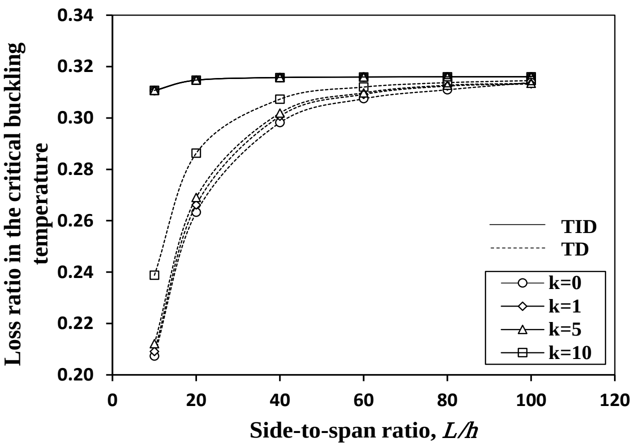

Fig. 9 Effect of side-to-thickness ratio on the loss ratio in the critical buckling temperature of ZrO_2/Ni with parabolic variation intensity $\xi = 2$.

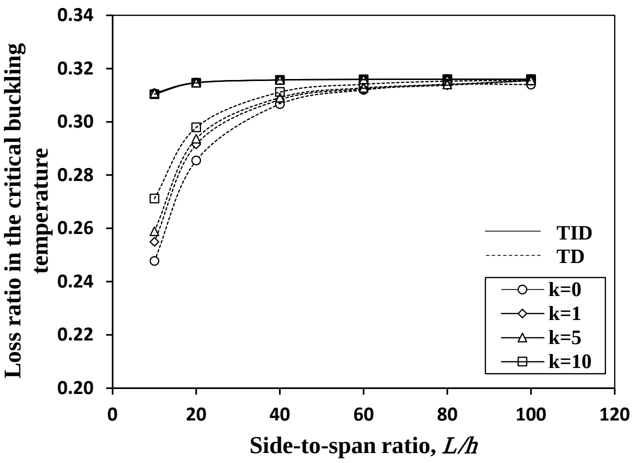

Fig. 10 Effect of side-to-thickness ratio on the loss ratio in the critical buckling temperature of SiN_4/ SUS304 with parabolic variation intensity$\xi = 2$

The relationship between the loss ratio in the thermal resistance and side-to-thickness ratio has been is plotted in Figs. 9 and 10 for ZrO_2/Ni and SiN_4/SUS304 beams, respectively with a fixed value of the parabolic variation intensity $\xi = 2$. It should be mentioned that the thickness h of the constant beam (when $\xi = 1$) is taken as reference represent the side-to-thickness L/h.

These figures illustrate that in case of considering that the material properties are independent on the temperature, the loss ratio in the buckling resistance of the beam is highly affected be the parabolic-variation of the thickness while no influence is observed of the aspect ratio (L/a) or the material properties. In this case, the loss ratio of the thermal buckling resistance of any FGM beam equals to about 31.5% when $\xi = 2$.

On the other hand, if the properties of the constituent materials are considered TD, the loss ratio of the thermal buckling resistance of the beam become highly sensitive to the material properties as well as geometric properties, especially for thick beams. However, this sensitivity decreases as L/a increases.

7. Conclusions

In this research work, the thermal stability of simply supported FGM beam is carried out in order to study the degradation in the thermal buckling resistance after varying the beam thickness according a parabolic-concave function. The material properties are considered dependent to the temperature change. The governing equation is solved numerically using finite difference method to have the ability to include the thickness variation. Effect of different geometrical and material properties on the buckling resistance of FGM beams are studied.

According to the obtained results, applying parabolic thickness variation to simply supported FGM beams with preserving their original material volume leads to the following main conclusions:

- The Exclusion of the temperature dependent material properties in the thermal analysis of FGM beams having critical thickness variation such as parabolic-concave variation results a significant overestimation of the critical buckling temperature of thick beams.
- In case of assuming that the material properties are independent on the temperature, the loss ratio in the buckling resistance of the beam is affected only by the geometric properties of the thickness variation. In this case, neither the aspect ratio (L/a) nor the material distribution variation influence the loss ratio in the buckling resistance of FGM beam (compared to the original beam which has constant thickness).
- On the other hand, including the material properties variation due to temperature change, the loss ratio in the thermal buckling resistance of the beam become highly sensitive to the material properties as well as geometric properties, especially for thick beams. However, this sensitivity decreases as L/a increases.

References

Abdelaziz, H.H., Ait Amar Meziane, M., Bousahla, A.A., Tounsi, A., Mahmoud, S.R. and Alwabli, A.S. (2017), "An efficient hyperbolic shear deformation theory for bending, buckling and free vibration of FGM sandwich plates with various boundary conditions", *Steel Compos. Struct., Int. J.*, **25**(6), 693-704.

Abualnour, M., Houari, M.S.A., Tounsi, A., Adda Bedia, E.A. and Mahmoud, S.R. (2018), "A novel quasi-3D trigonometric plate theory for free vibration analysis of advanced composite plates", *Compos. Struct.*, **184**, 688-697.

Ahmed, A. (2014), "Post buckling analysis of sandwich beams with functionally graded faces using a consistent higher order theory", *Int. J. Civil, Struct. Envir.*, **4**(2), 59-64.

Ait Amar Meziane, M., Abdelaziz, H.H. and Tounsi, A. (2014), "An efficient and simple refined theory for buckling and free vibration of exponentially graded sandwich plates under various boundary conditions", *J Sandw. Struct. Mater.*, **16**(3), 293-318.

Ait Yahia, S., Ait Atmane, H., Houari, M.S.A. and Tounsi, A. (2015), "Wave propagation in functionally graded plates with porosities using various higher-order shear deformation plate theories", *Struct. Eng. Mech., Int. J.*, **53**(6), 1143-1165.

Akavci, S.S. (2015), "An efficient shear deformation theory for free vibration of functionally graded thick rectangular plates on elastic foundation", *Compos. Struct.*, **108**, 667-676.

Akbaş, Ş.D. (2015), "Wave propagation of a functionally graded beam in thermal environments", *Steel Compos. Struct., Int. J.*, **19**(6), 1421-1447.

Anandrao, K., Gupta, R., Ramachandran, P. and Rao, G. (2013), "Thermal buckling and free vibration analysis of heated functionally graded material beams", *Defence Sci. J.*, **63**(3), 315-322.

Arani, A.J. and Kolahchi, R. (2016), "Buckling analysis of embedded concrete columns armed with carbon nanotubes", *Comput. Concrete*, **17**(5), 567-578.

Atmane H., Tounsi A., Ziane N. and Mechab I., (2011), "Mathematical Solution For Free Vibration of Sigmoid Functionally Graded Beams With Varying Cross-Section", *Steel Compos. Struct., Int. J.*, **11**(6), 489-504.

Attia, A., Bousahla, A.A., Tounsi, A., Mahmoud, S.R. and Alwabli, A.S. (2018), "A refined four variable plate theory for thermoelastic analysis of FGM plates resting on variable elastic foundations", *Struct. Eng. Mech., Int. J.*, **65**(4), 453-464.

Aydogdu, M. (2006), "Buckling analysis of cross-ply laminated beams with general boundary conditions by ritz method", *Compos. Sci. Technol.*, **66**(10), 1248-1255.

Belabed, Z., Houari, M.S.A., Tounsi, A., Mahmoud, S.R. and Anwar Bég, O. (2014), "An efficient and simple higher order shear and normal deformation theory for functionally graded material (FGM) plates", *Compos. Part B*, **60**, 274-283.

Belabed, Z., Bousahla, A.A., Houari, M.S.A., Tounsi, A. and Mahmoud, S.R. (2018), "A new 3-unknown hyperbolic shear deformation theory for vibration of functionally graded sandwich plate", *Earthq. Struct.*, **14**(2), 103-115.

Beldjelili, Y., Tounsi, A. and Mahmoud, S.R. (2016), "Hygro-thermo-mechanical bending of S-FGM plates resting on variable elastic foundations using a four-variable trigonometric plate theory", *Smart Struct. Syst., Int. J.*, **18**(4), 755-786.

Bellifa, H., Bakora, A., Tounsi, A., Bousahla, A.A. and Mahmoud, S.R. (2017), "An efficient and simple four variable refined plate theory for buckling analysis of functionally graded plates", *Steel Compos. Struct., Int. J.*, **25**(3), 257-270.

Bennai, R., Atmane, H. and Tounsi, A. (2015), "A new higher-order shear and normal deformation theory for functionally graded sandwich beams", *Steel Compos. Struct., Int. J.*, **19**(3), 521-546.

Bennoun, M., Houari, M.S.A. and Tounsi, A. (2016), "A novel five variable refined plate theory for vibration analysis of functionally graded sandwich plates", *Mech. Adv. Mater. Struct.*, **23**(4), 423-431.

Bilouei, B.S., Kolahchi, R. and Bidgoli, M.R. (2016), "Buckling of concrete columns retrofitted with Nano-Fiber Reinforced Polymer (NFRP)", *Comput. Concrete*, **18**(5), 1053-1063.

Bouazza, M., Amara, K., Zidour, M., Tounsi, A. and Adda-Bedia, E.A. (2014), "Hygrothermal effects on the postbuckling response of composite beams", *Am. J. Mater. Res.*, **1**(2), 35-43.

Bouderba, B., Houari, M.S.A. and Tounsi, A. and Mahmoud, S.R. (2016), "Thermal stability of functionally graded sandwich plates using a simple shear deformation theory", *Struct. Eng. Mech., Int. J.*, **58**(3), 397-422.

Bouguenina, O., Belakhdar, K., Tounsi, A. and Adda-Bedia, E.A. (2015), "Numerical analysis of FGM plates with variable thickness subjected to thermal buckling", *Steel Compos. Struct., Int. J.*, **19**(3), 679-695.

Bousahla, A.A., Benyoucef, S., Tounsi, A. and Mahmoud, S.R. (2016), "On thermal stability of plates with functionally graded coefficient of thermal expansion", *Struct. Eng. Mech., Int. J.*, **60**(2), 313-335.

De Faria, A. and De Almeida, S.M. (2004), "Buckling optimization of variable thickness composite plates subjected to non uniform loads", *AIAA J.*, **42**(2), 228-231.

El-Haina, F., Bakora, A., Bousahla, A.A., Tounsi, A. and Mahmoud, S.R. (2017), "A simple analytical approach for thermal buckling of thick functionally graded sandwich plates", *Struct. Eng. Mech., Int. J.*, **63**(5), 585-595.

Fallah, A. and Aghdam, M. (2012), "Thermo-mechanical buckling and nonlinear free vibration analysis of functionally graded beams on nonlinear elastic foundation", *Compos. Part B-Eng.*, **43**(3), 1523-1530.

Ghayesh, M.H. and Farokhi, H. (2018), "Bending and vibration analyses of coupled axially functionally graded tapered beams", *Nonlinear Dyn.*, **91**(1), 17-28.

Ghomshei, M. and Abbasi, V. (2013), "Thermal buckling analysis of annular FGM plate having variable thickness under thermal load of arbitrary distribution by finite element method", *J. Mech. Sci. Technol.*, **27**(4), 1031-1039.

Hadji, L., Zouatnia, N. and Kassoul, A. (2017), "Wave propagation in functionally graded beams using various higherorder shear deformation beams theories", *Struct. Eng. Mech., Int. J.*, **62**(2), 143-149.

Hajmohammad, M.H., Zarei, M.S., Nouri, A. and Kolahchi, R. (2017), "Dynamic buckling of sensor/functionally graded-carbon nanotube-reinforced laminated plates/actuator based on sinusoidal-visco-piezoelasticity theories", *J. Sandw. Struct. Mater.*, 1099636217720373.

Hebali, H., Tounsi, A., Houari, M.S.A., Bessaim, A. and Adda Bedia, E.A. (2014), "A new quasi-3D hyperbolic shear deformation theory for the static and free vibration analysis of functionally graded plates", *ASCE J. Eng. Mech.*, **140**, 374-383.

Huang, Y. and Li, X. (2010), "Buckling of functionally graded circular columns including shear deformation", *Mater. Des.*, **31**(7), 3159-3166.

Jabbarzadeh, M., Eskandari, J. and Khosravi, M. (2013), "The analysis of thermal buckling of circular plates of variable thickness from functionally graded materials", *Modares Mech. Eng.*, **12**(5), 59-73.

Janghorban, M. and Rostamsowlat, I. (2012), "Free vibration analysis of functionally graded plates with multiple circular and non-circular cutouts", *Chinese J. Mech. Eng.*, **25**(2), 277-284.

Kaci, A., Houari, M.S.A., Bousahla, A.A., Tounsi, A. and Mahmoud, S.R. (2018), "Post-buckling analysis of shear-deformable composite beams using a novel simple two-unknown beam theory", *Struct. Eng. Mech., Int. J.*, **65**(5), 621-631.

Kar, V.R. and Panda, S.K. (2015), "Nonlinear flexural vibration of shear deformable functionally graded spherical shell panel", *Steel Compos. Struct., Int. J.*, **18**(3), 693-709.

Kar, V.R. and Panda, S.K. (2016), "Post-buckling behaviour of shear deformable functionally graded curved shell panel under edge compression", *Int. J. Mech. Sci.*, **115**, 318-324.

Kar, V.R. and Panda, S.K. (2017), "Postbuckling analysis of shear deformable FG shallow spherical shell panel under nonuniform thermal environment", *J. Therm. Stress.*, **40**(1), 25-39.

Karami, B., Shahsavari, D. and Janghorban, M. (2017a), "Wave propagation analysis in functionally graded (FG) nanoplates under in-plane magnetic field based on nonlocal strain gradient theory and four variable refined plate theory", *Mech. Adv. Mater. Struct.*, 1-11.

Karami, B., Shahsavari, D. and Li, L. (2017b), "Temperature-dependent flexural wave propagation in nanoplate-type porous heterogenous material subjected to in-plane magnetic field", *J. Therm. Stress.*, 1-17.

Karami, B., Janghorban, M. and Li, L. (2018a), "On guided wave propagation in fully clamped porous functionally graded nanoplates", *Acta Astronaut.*, **143**, 380-390.

Karami, B., Shahsavari, D., Li, L., Karami, M. and Janghorban, M. (2018b) "Thermal buckling of embedded sandwich piezoelectric nanoplates with functionally graded core by a nonlocal second-order shear deformation theory", *Proc. Inst. Mech. Eng. Part C - J. Mech. Eng. Sci.*, 954406218756451.

Katariya, P.V. and Panda, S.K. (2016), "Thermal buckling and vibration analysis of laminated composite curved shell panel", *Aircr. Eng. Aerosp. Technol. An Int. J.*, **88**(1), 97-107.

Katariya, P.V., Panda, S.K., Hirwani, C.K., Mehar, K. and Thakare, O. (2017), "Enhancement of thermal buckling strength of laminated sandwich composite panel structure embedded with shape memory alloy fibre", *SMART Struct. Syst.*, **20**(5), 595-605.

Kiani, Y. and Eslami, M.R. (2010), "Thermal buckling analysis of functionally graded material beams", *Int. J. Mech. Sci. Mater. Des.*, **6**(3), 229-238.

Kiani, Y. and Eslami, M. (2013), "Thermomechanical buckling of temperature-dependent FGM beams", *Latin Am. J. Solids Struct.*, **10**(2), 223-246.

Kolahchi, R. (2017), "A comparative study on the bending, vibration and buckling of viscoelastic sandwich nano-plates based on different nonlocal theories using DC, HDQ and DQ methods", *Aerosp. Sci. Technol.*, **66**, 235-248.

Kolahchi, R. and Bidgoli, A.M.M. (2016), "Size-dependent sinusoidal beam model for dynamic instability of single-walled carbon nanotubes", *Appl. Math. Mech.*, **37**(2), 265-274.

Kolahchi, R. and Cheraghbak, A. (2017), "Agglomeration effects on the dynamic buckling of viscoelastic microplates reinforced with SWCNTs using Bolotin method", *Nonlinear Dyn.*, **90**(1), 479-492.

Kolahchi, R., Hosseini, H. and Esmailpour, M. (2016a), "Differential cubature and quadrature-Bolotin methods for dynamic stability of embedded piezoelectric nanoplates based on visco-nonlocal-piezoelasticity theories", *Compos. Struct.*, **157**, 174-186.

Kolahchi, R., Safari, M. and Esmailpour, M. (2016b), "Dynamic stability analysis of temperature-dependent functionally graded CNT-reinforced visco-plates resting on orthotropic elastomeric medium", *Compos. Struct.*, **150**, 255-265.

Kolahchi, R., Keshtegar, B. and Fakhar, M.H. (2017a), "Optimization of dynamic buckling for sandwich nanocomposite plates with sensor and actuator layer based on sinusoidal-visco-piezoelasticity theories using Grey Wolf algorithm", *J. Sandw. Struct. Mater.*, 1099636217731071.

Kolahchi, R., Zarei, M.S., Hajmohammad, M.H. and Oskouei, A.N. (2017b), "Visco-nonlocal-refined Zigzag theories for dynamic buckling of laminated nanoplates using differential cubature-Bolotin methods", *Thin-Wall. Struct.*, **113**, 162-169.

Kolahchi, R., Zarei, M.S., Hajmohammad, M.H. and Nouri, A. (2017c), "Wave propagation of embedded viscoelastic FG-CNT-reinforced sandwich plates integrated with sensor and actuator based on refined zigzag theory", *Int. J. Mech. Sci.*, **130**, 534-545.

Madani, H., Hosseini, H. and Shokravi, M. (2016), "Differential cubature method for vibration analysis of embedded FG-CNT-reinforced piezoelectric cylindrical shells subjected to uniform and non-uniform temperature distributions", *Steel Compos. Struct., Int. J.*, **22**(4), 889-913.

Menasria, A., Bouhadra, A., Tounsi, A., Bousahla, A.A. and Mahmoud, S.R. (2017), "A new and simple HSDT for thermal stability analysis of FG sandwich plates", *Steel. Compos. Struct., Int. J.*, **25**(2), 157-175.

Mohammadabadi, M., Daneshmehr, A. and Homayounfard, M. (2015), "Size-dependent thermal buckling analysis of micro composite laminated beams using modified couple stress theory", *Int. J. Eng. Sci.*, **92**, 47-62.

Mozafari, H. and Ayob, A. (2012), "Effect of thickness variation on the mechanical buckling load in plates made of functionally graded materials", *Procedia Tech*, **1**, 496-504.

Mozafari, H., Ayob, A. and Alias, A. (2010), "Influence of thickness variation on the buckling load in plates made of functionally graded materials", *Eur. J. Sci. Res.*, **47**(3), 422-435.

Nami, M.R., Janghorban, M. and Damadam, M. (2015), "Thermal buckling analysis of functionally graded rectangular nanoplates based on nonlocal third-order shear deformation theory", *Aerosp. Sci. Technol.*, **41**, 7-15.

Panda, S.K. and Katariya, P.V. (2015), "Stability and free vibration behaviour of laminated composite panels under thermo-mechanical loading", *Int. J. Appl. Comput. Math.*, **1**(3), 475-490.

Panda, S.K. and Singh, B.N. (2009), "Thermal post-buckling behaviour of laminated composite cylindrical/hyperboloid shallow shell panel using nonlinear finite element method", *Compos. Struct.*, **91**(3), 366-374.

Panda, S.K. and Singh, B.N. (2010), "Thermal post-buckling analysis of a laminated composite spherical shell panel embedded with shape memory alloy fibres using non-linear finite element method", *Proc. Inst. Mech. Eng. Part C - J. Mech. Eng. Sci.*, **224**(4), 757-769.

Panda, S.K. and Singh, B.N. (2013a), "Large amplitude free vibration analysis of thermally post-buckled composite doubly curved panel embedded with SMA fibers", *Nonlinear Dyn.*, **74**(1-2), 395-418.

Panda, S.K. and Singh, B.N. (2013b), "Nonlinear finite element analysis of thermal post-buckling vibration of laminated composite shell panel embedded with SMA fibre", *Aerosp. Sci. Technol.*, **29**(1), 47-57.

Panda, S.K. and Singh, B.N. (2013c), "Post-buckling analysis of laminated composite doubly curved panel embedded with SMA fibers subjected to thermal environment", *Mech. Adv. Mater. Struct.*, **20**(10), 842-853.

Panda, S.K. and Singh, B.N. (2013d), "Thermal Postbuckling Behavior of Laminated Composite Spherical Shell Panel Using NFEM#", *Mech. Based Des. Struct. Mach.*, **41**(4), 468-488.

Pouladvand, M. (2009), "Thermal stability of thin rectangular plates with variable thickness made of functionally graded material", *J. Solid. Mech.*, **1**(3), 171-189.

Rajasekaran, S. and Wilson, A. (2013), "Buckling and vibration of rectangular plates of variable thickness with different end conditions by finite difference technique", *Struct. Eng. Mech., Int. J.*, **46**(2), 269-294.

Robert, M.J. (2006), "Buckling of bars plates and shells", Bull Ridge.

Shahsavari, D., Shahsavarib, M., Li, L. and Karami, B. (2018), "A novel quasi-3D hyperbolic theory for free vibration of FG plates with porosities resting on Winkler/Pasternak/Kerr foundation", *Aerosp. Sci. Technol.*, **72**, 134-149.

Shahsiah, R., Nikbin, K.M. and Eslami, M.R. (2009), "Thermal buckling of functionally graded beams", *Iran J. Mech. Eng.*, **10**(2), 64-80.

Shen, H. (2009), *Functionally Graded Materials: Non-linear Analysis of Plates and Shells*, CRC Press, New York, NY, USA.

Shokravi, M. (2017a), "Buckling analysis of embedded laminated plates with agglomerated CNT-reinforced composite layers using FSDT and DQM", *Geomech. Eng., Int. J.*, **12**(2), 327-346.

Shokravi, M. (2017b), "Buckling of sandwich plates with FG-CNT-reinforced layers resting on orthotropic elastic medium using Reddy plate theory", *Steel Compos. Struct., Int. J.*, **23**(6), 623-631.

Shokravi, M. (2017c), "Dynamic pull-in and pull-out analysis of viscoelastic nanoplates under electrostatic and Casimir forces via sinusoidal shear deformation theory", *Microelectron. Reliab.*, **71**, 17-28.

Shokravi, M. (2017d), "Vibration analysis of silica nanoparticles-reinforced concrete beams considering agglomeration effects", *Comput. Concrete*, **19**(3), 333-338.

Siddiqui, F. (2015), "Extended higher order theory for sandwich plates of arbitrary aspect ratio", Thesis; Georgia Institute of Technology.

Sun, Y., Li, S. and Batra, R. (2016), "Thermal buckling and post-buckling of FGM Timoshenko beams on nonlinear elastic foundation", *J. Therm. Stresses*, **39**(1), 11-26.

Szilard, R. (2004), *Theories and Applications of Plate Analysis: Classical Numerical and Engineering Methods*, John Wiley & Sons, USA.

Wattanasakulpong, N., Gangadhara, P.B. and Kelly, D. (2011), "Thermal buckling and elastic vibration of third-order shear deformable functionally graded beams", *Int. J. Mech. Sci.*, **53**(9), 734-743.

Yazdani, S., Kiani, Y., Jabbari, M. and Eslami, M. (2011), "Thermal buckling of piezoelectric composite beam", *ISRN Mech. Eng.*, **2011**, 1-11.

Zamanian, M., Kolahchi, R. and Bidgoli, M.R. (2017), "Agglomeration effects on the buckling behaviour of embedded concrete columns reinforced with SiO_2 nano-particles", *Wind Struct., Int. J.*, **24**(1), 43-57.

CC